

Ground-state properties of the electron-hole liquid in Ge under $\langle 111 \rangle$ uniaxial stress

G. Kirczenow and K. S. Singwi

Department of Physics and Astronomy, Northwestern University, Evanston, Illinois 60201

(Received 28 August 1978)

We present a calculation of the ground-state energy E_g , density n , and electron and hole Fermi energy $E_F(E)$, $E_F(H)$ of the electron-hole drop in $\langle 111 \rangle$ -stressed Ge using two different models for the exchange-correlation energy. Good agreement is found with experiment. The experimentally observed increase of the electron Fermi energy with stress at low stress is explained by our calculation, and an interesting very rapid and possibly discontinuous variation of n , $E_F(E)$, and $E_F(H)$ with stress associated with the emptying of the hot conduction valleys is predicted.

I. INTRODUCTION

The band structure of unstressed Ge has four equivalent conduction-band minima at the zone boundary and a doubly degenerate valence-band maximum at the zone center. When a $\langle 111 \rangle$ uniaxial stress is applied to the crystal these degeneracies are lifted. The valence-band maximum is split into two bands which are only spin degenerate and one of the conduction valleys becomes lower than the others. If the stress is very large the two hole bands decouple and their constant-energy surfaces near to the zone center become simple ellipsoids. Thus in the limit of very large $\langle 111 \rangle$ stress the calculation of the properties of the electron-hole liquid (EHL) in Ge becomes much simpler than in the unstressed case. This was noted by Combescot and Nozières¹ and Brinkman and Rice,² and a sophisticated calculation of the electron-hole drop (EHD) ground-state properties in the limit of large $\langle 111 \rangle$ stress was made by Vashishta *et al.*³ who predicted that the EHD should exist in this limit as well as at zero stress.

Partly in order to test the accuracy of this calculation a number of experiments on the EHD in uniformly $\langle 111 \rangle$ -stressed Ge have recently been performed and many interesting experimental data have been obtained. The ground-state properties of the EHD have been measured.⁴⁻⁶ Chou and Wong⁶ have also been able to verify the density dependence of the many-body enhancement of the electron-hole pair correlation function $g_{eh}(0)$ in the EHD which was calculated by Vashishta *et al.*³ by interpreting the results of their stress-dependent experiments. In addition, recently the presence of nonequilibrium "hot" electrons (in the three conduction valleys which are raised in energy by $\langle 111 \rangle$ stress) in the EHD has been reported.⁷⁻⁹

In an earlier paper¹⁰ we gave a calculation of the properties of the EHD in which these electrons in the "hot" valleys are assumed to decay very slowly into the cold valley so that the hot and cold elec-

trons could be treated as separate species in thermal quasiequilibrium, but usually having different Fermi levels and chemical potentials. We predicted that at $T=0$ and certain values of stress such an EHD would phase separate into two distinct degenerate Fermi liquids.

In this article we consider the opposite limit to that discussed in Ref. 10. Namely, we consider the situation where the electrons in all of the valleys are in true equilibrium with each other so that at $T=0$ either there are no electrons in the three upshifted valleys or otherwise (if the stress splitting of the conduction band is small enough) the pair chemical potential of the electrons in the higher-energy ("hot") valleys is equal to that of the electrons in the lower ("cold") valley. This situation can be achieved experimentally either by waiting for a sufficient time after the EHD is created by a laser pulse in a perfect Ge crystal so that the electrons in the hot and cold valleys have come into equilibrium with each other by electron-electron intervalley scattering,^{6,7,9} or by using a very lightly doped sample, since the presence of even a rather low concentration of impurities in the crystal greatly reduces the intervalley scattering time.⁹

Preliminary theoretical results for this case, which we will refer to as the equilibrium limit (EL), at $T=0$ have been published by Markiewicz and Kelso¹¹ and by Liu.¹² Although it has been possible experimentally to attain stresses large enough that in the EL only one conduction and one valence valley are occupied by electrons and holes, respectively, these calculations showed that the values of stress which have so far been achieved are not sufficiently high for the large-stress limit in the sense of the calculation of Vashishta *et al.*³ to apply because of the nonparabolicity and warping of the stress-split valence band. However, a systematic theoretical treatment of the stress dependence of the EHD in the EL and particularly of the low-stress region in which there are electrons in both the hot and the

cold valleys has been lacking. Markiewicz and Kelso¹¹ did extend their treatment to low stress but used a model in which only one conduction valley is occupied by electrons so that effects due to the presence of electrons in the hot valleys at low stress were not included.

Here we present a detailed study of the dependence on $\langle 111 \rangle$ stress of the ground-state energy, density, and electron and hole Fermi energies of the EHD in the EL at $T=0$ in Ge. The hole kinetic energy is calculated including the nonparabolicity and warping of both stress-split valence bands according to the $\vec{k} \cdot \vec{p}$ formalism of Pikus and Bir.¹³ The electron kinetic energy is calculated including the effects of populating both the hot and cold valleys at those lower values of stress for which this is appropriate. The exchange-correlation energy is calculated by using the near independence of this quantity on details of band structure as discussed in Ref. 10. Two models, which can be considered as opposite limiting cases, are used for the exchange-correlation energy and good agreement is found with the available experimental data.

A number of new and interesting features of this system are revealed by our calculation. We find that at very low stress both the electron and hole Fermi energies increase initially as the stress is increased despite the fact that the carrier density in the EHD is at the same time decreasing. This effect occurs because as the stress splitting of the conduction band increases it is energetically favorable for some of the electrons from the hot valleys to "spill over" into the cold valley as the hot valleys are upshifted by the stress, and similarly for the two hole bands. For the electrons this calculated increase of the Fermi energy is quite strong and has been observed experimentally. Another new qualitative result is that as the value of the stress is increased through the region in which the hot valleys are emptied of electrons, the electron and hole Fermi energies and also the EHD density all decrease by a large fraction over a very narrow range of stress values, and possibly even change discontinuously with stress. However, in the range of stress values in which this is expected to occur the presently available experimental data is not accurate enough to test this prediction.

II. BAND STRUCTURE

The system which we are considering contains N_c electrons in the cold valley, N_h electrons distributed equally among the three hot valleys and N_{\pm} holes occupying the two stress-split valence bands. We label the latter (+) and (-) according to the hole energy-dispersion relation of Pikus and

Bir.¹³ For a $\langle 111 \rangle$ stress this can be written in the form

$$E_{\pm}(\vec{k}) = A k^2 \pm [F(\theta, \varphi) k^4 + \frac{1}{2} G(\theta) k^2 S_H + \frac{1}{4} S_H^2]^{1/2} + \frac{1}{2} S_H, \quad (1)$$

where

$$F(\theta, \varphi) = B^2 + C^2 [\frac{1}{3} \cos^4 \theta + \frac{1}{4} \sin^4 \theta - (\sqrt{2}/3) \sin^3 \theta \cos \theta \sin 3\phi], \quad (2)$$

$$G(\theta) = (B^2 + \frac{1}{3} C^2)^{1/2} (1 - 3 \cos^2 \theta). \quad (3)$$

The angles θ and φ refer to the $\langle 111 \rangle$ stress axis, S_H is the stress splitting of the valence band at $\vec{k} = 0$ (note that the quantity Δ used by Liu¹² is equal to $\frac{1}{2} S_H$), and A , B , and C are constants (see Table I) which have been taken from Hensel and Suzuki.¹⁴ The electron dispersion

$$E_{h,c}(\vec{k}) = \frac{\hbar^2}{2} \left(\frac{k_l^2}{m_l} + \frac{k_t^2}{m_t} \right) + S_E \alpha_{h,c} \quad (4)$$

is used for each valley where l and t refer to longitudinal and transverse components, respectively, S_E is the stress splitting of the conduction band, $\alpha_c = 0$, and $\alpha_h = 1$.

The EHD energy E depends on N_h , N_c , N_+ , N_- , and V where V is the volume. We calculate the electron and hole kinetic energy from the relations (1)–(4) without any further approximations, the hole bands $E_{\pm}(\vec{k})$ being treated numerically as explained below.

The exchange-correlation energy E_{xc} for this system would require an excessive amount of computer time to calculate from first principles because of the strong nonparabolicity, warping, and coupling of the stress-split hole bands in the region of stresses of interest and because of the multicomponent nature of the system. Thus, we prefer to exploit the fact that E_{xc} is not sensitive to such details of band structure as how the electrons are distributed among a number of different conduction valleys or the holes among valence bands, or to band anisotropy, i.e., E_{xc} is sensitive only to the total electron (or hole) density in the EHD. As illustrated in Ref. 10, while these band-structure features can affect the separate exchange and correlation contributions quite strongly, the effect on the sum E_{xc} appears to be very weak. While it is easy to demonstrate that the band-

TABLE I. Ge parameters used in the calculation. Valence-band parameters A, B, C taken from Ref. 14.

A	B	C	m_l	m_t	S_E/S_H	R_y
13.38	8.48	13.15	0.082	1.58	2.8	2.655 meV

structure effects on exchange and correlation should tend to cancel in the sum, the accuracy of the cancellation found in practice is surprisingly good. We know of no general theorem which would require such a detailed cancellation. It should be noted as well that when Vashishta *et al.*³ calculated the correlation energy for an electron-hole liquid with simple, parabolic electron and hole bands this was found to be insensitive to the electron-hole mass ratio. Since the exchange does not depend on mass, this is another example of the lack of sensitivity of E_{xc} to band structure. Thus, as in Ref. 10, we will approximate the exchange-correlation energy of the EHD by choosing a simple model system and using the exchange-correlation energy for that model system as a function of the electron density to represent the exchange-correlation energy of the EHD in $\langle 111 \rangle$ -stressed Ge at the same total electron or hole density n .

$$n = n_h + n_c = n_+ + n_- \quad (5)$$

where n stands for N/V . We will use two different extreme case models for this purpose. (a) An exchange-correlation energy E_{xc}^0 which corresponds to a "zero-stress" model band structure with four spherically symmetrical conduction valleys and two decoupled spherical valence bands of equal mass equally populated with electrons and holes, respectively. [This is model I in the notation of Bhattacharyya *et al.*,¹⁵ and we use the numerical correlation energies which they label SPH (self-consistent particle-hole approximation).] (b) An exchange-correlation energy E_{xc}^∞ which corresponds to the limiting Ge band structure at large $\langle 111 \rangle$ stress, i.e., only one ellipsoidal conduction valley and one ellipsoidal hole band are populated. (For this model we use the numerical correlation energy listed by Vashishta *et al.*³ under "Ge $\langle 111 \rangle$ fully self-consistent anisotropic.")

III. EQUILIBRIUM LIMIT

If one makes the above approximation that the exchange-correlation energy (per pair) depends only on the total electron density, the energy E of the EHD relative to the stressed Ge band gap can be written

$$\begin{aligned} E(N_h, N_c, N_+, N_-, V) &= E^h(N_h, V) + E^c(N_c, V) \\ &+ E^+(N_+, V) + E^-(N_-, V) \\ &+ E_{xc}(N, V), \end{aligned} \quad (6)$$

where E^h, E^c, E^+, E^- are the kinetic energies (including stress splittings) of the particles in the respective bands. Or in terms of the respective

densities of states, Z^h, Z^c, Z^+, Z^- and Fermi energies $E_F^h, E_F^c, E_F^+, E_F^-$:

$$\begin{aligned} E(N_h, N_c, N_+, N_-, V) &= \int_{S_E}^{E_F^h + S_E} E Z^h(E) dE \\ &+ \int_0^{E_F^c} E Z^c(E) dE \\ &+ \int_{S_H}^{E_F^+ + S_H} E Z^+(E) dE \\ &+ \int_0^{E_F^-} E Z^-(E) dE + E_{xc}(N, V). \end{aligned} \quad (7)$$

Note that E_F^i is defined to be zero if N_i is zero, i.e., the Fermi energy is measured relative to the edge of the respective electron (h or c) or hole ($+$ or $-$) band. Because of charge neutrality [Eq. (5)], this system is described by four pair chemical potentials which at $T=0$ are defined to be

$$\begin{aligned} \mu_{h+} &\equiv \left(\frac{\partial E}{\partial N_h} \right)_{V, N_c, N_-} \quad (N_h + N_c = N_+ + N_-) \\ &= E_F^h + S_E + E_F^+ + S_H + \mu_{xc}(n), \\ \mu_{h-} &\equiv \left(\frac{\partial E}{\partial N_h} \right)_{V, N_c, N_+} \quad (N_h + N_c = N_+ + N_-) \\ &= E_F^h + S_E + E_F^- + \mu_{xc}(n), \\ \mu_{c+} &\equiv \left(\frac{\partial E}{\partial N_c} \right)_{V, N_h, N_-} \quad (N_h + N_c = N_+ + N_-) \\ &= E_F^c + E_F^+ + S_H + \mu_{xc}(n), \\ \mu_{c-} &\equiv \left(\frac{\partial E}{\partial N_c} \right)_{V, N_h, N_+} \quad (N_h + N_c = N_+ + N_-) \\ &= E_F^c + E_F^- + \mu_{xc}(n), \end{aligned} \quad (8)$$

where

$$\mu_{xc}(n) = \left(\frac{\partial E_{xc}}{\partial N} \right)_V \quad (9)$$

and the derivatives in (8) are taken keeping the number of holes of one type fixed and varying the number of holes of the other type in such a way as to always preserve charge neutrality. In the equilibrium limit the hot and cold electrons are in equilibrium with each other as are the holes of the two bands. In the case when all bands are occupied this implies that

$$\mu_{h+} = \mu_{h-} = \mu_{c+} = \mu_{c-} \quad (10)$$

If N_h or N_+ or both are zero then only those equalities of (10) hold for which *all* of the species in-

volved have nonzero populations. Then from (8) and (10),

$$E_F^h = \begin{cases} E_F^c - S_E, & \text{if } N_h > 0 \\ 0, & \text{otherwise;} \end{cases} \quad (11)$$

$$E_F^+ = \begin{cases} E_F^- - S_H, & \text{if } N_+ > 0 \\ 0, & \text{otherwise.} \end{cases} \quad (12)$$

Thus in the EL we will work in terms of a single-electron Fermi energy $E_F(E) \equiv E_F^c$ and a single-hole Fermi energy $E_F(H) \equiv E_F^+$; the connection with description in terms of two-electron and two-hole bands via (11) and (12) will be understood.

It should be emphasized that although Eq. (10) is exact in the EL, Eqs. (11) and (12) are a consequence of our approximation that E_{xc}/N depends only on the total EHD density and *not* on the way in which the electrons and holes are distributed among the various bands. Consequently (11) and (12) are also only approximately valid. This should be born in mind in fitting experimental luminescence spectra with Fermi-function convolutions. For example, it may turn out to be useful to replace S_E and S_H in (11) and (12) by S'_E and S'_H which

depend on the occupation of the various bands, i.e., to introduce a many-body renormalization of the conduction- and valence-band stress splitting. However, we will not pursue that refinement in this paper but will continue to use (11) and (12) and $E_F(E)$ and $E_F(H)$ as defined above.

With the constraints (11) and (12), at $T=0$, the energy per pair, $E = E(N_h, N_c, N_+, N_-, V)/N$ at a given stress is a function only of the total density n and its minimization gives the EHD ground state. Given (11), calculation of the electron kinetic energy contribution to ϵ is trivial. Our numerical evaluation of the hole kinetic energy is outlined in the next section.

IV. HOLE KINETIC ENERGY AND DENSITY

We find it convenient to calculate the total hole density $n = n_+ + n_-$ and kinetic energy $\epsilon^H = [E^-(N_-, V) + E^+(N_+, V)]/N$ numerically as a function of $E_F(H)$, and then by an interpolation procedure to obtain ϵ^H for any desired hole density.

To do this note that the hole energy-dispersion relation (1) can be inverted to yield k as a function of E_{\pm} for any fixed θ and φ :

$$k_{\pm}^2(E) = \{2A\chi + \frac{1}{2}GS_H \mp [(2A\chi + \frac{1}{2}GS_H)^2 - 4(A^2 - F)(\chi^2 - \frac{1}{4}S_H^2)]^{1/2}\}/2(A^2 - F), \quad (13)$$

where $\chi = E - \frac{1}{2}S_H$ and the arguments θ and φ of F , G , and k_{\pm} are understood. By setting $E_F(H)$ for E in (13) the hole Fermi surface in \vec{k} space is obtained.

Then

$$\begin{aligned} n(E_F(H)) &= \frac{2}{(2\pi)^3} \left(\int_{|\vec{k}| \leq k_+(E_F(H))} d^3k \right. \\ &\quad \left. + \int_{|\vec{k}| \leq k_-(E_F(H))} d^3k \right) \\ &= \frac{1}{12\pi^3} \int_0^{2\pi} \int_0^{\pi} \sin\theta d\varphi d\theta [k_+^3(\theta, \varphi, E_F(H)) \\ &\quad + k_-^3(\theta, \varphi, E_F(H))]; \end{aligned} \quad (14)$$

$$\begin{aligned} \epsilon^H(E_F(H)) &= \frac{2}{(2\pi)^3 n(E_F(H))} \left(\int_{|\vec{k}| \leq k_+(E_F(H))} E_+(\vec{k}) d^3k \right. \\ &\quad \left. + \int_{|\vec{k}| \leq k_-(E_F(H))} E_-(\vec{k}) d^3k \right). \end{aligned} \quad (15)$$

It is easy to show that ϵ^H and n can be written in the form

$$\epsilon^H = E_F(H) f_{\epsilon}(R), \quad (16)$$

$$n = [E_F(H)]^{3/2} f_n(R), \quad (17)$$

where

$$R = E_F(H)/S_H. \quad (18)$$

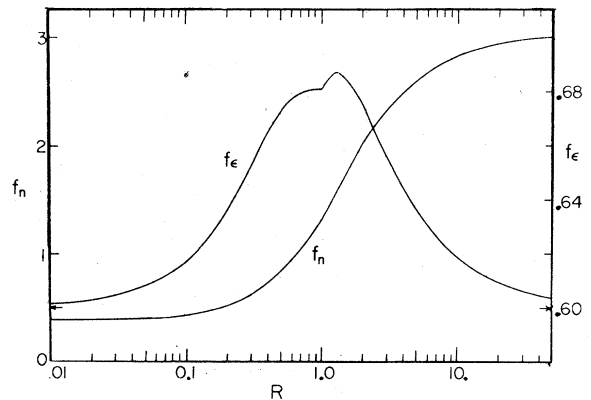


FIG. 1. Hole energy and density scaling factors f_{ϵ} and f_n (in units of $10^{22} \text{ m}^{-3} \text{ meV}^{-1.5}$) vs $R = E_F(H)/S_H$.

This factorization has the advantage that once f_n and f_ϵ have been computed as a function of R they can be used to obtain ϵ^H and n at any stress.

The quantities f_ϵ and f_n were calculated numerically from the expressions (14) and (15) at intervals of 5% in R over the range of interest. A finer mesh was used close to $R=1$. The numerical accuracy was better than 0.1%. The results are shown in Fig. 1. Since as $R \rightarrow 0$ or ∞ the hole density of states becomes parabolic and approaches a finite limit, both f_ϵ and f_n tend to finite values in these limits. Note that $f_\epsilon \rightarrow \frac{2}{3}$ as it should in both limits. The change in slope at $R=1$ of both f_ϵ and f_n is due to the entry of the (+) hole band. Liu and Liu¹⁶ have pointed out that the hole density of states is approximately linear over a wide range of hole energies which are smaller than S_H and used this linearity to calculate the EHD critical point in the EL. This linear approximation yields $f_\epsilon = \frac{2}{3}$ which is in rough agreement with our calculation at intermediate values of R .

V. CALCULATIONS AND RESULTS

At any given stress ϵ^H and n were calculated numerically as a function of $E_F(H)$ using (16)–(18) and a cubic spline interpolation was used to find ϵ^H as a function of n . The electron kinetic energy was evaluated for the band structure given by (4) using the relation (11) between the hot- and cold-electron Fermi energies. Since we measure the stress by the energy splitting S_H of the two valence bands it is necessary to know the ratio S_E/S_H which we take

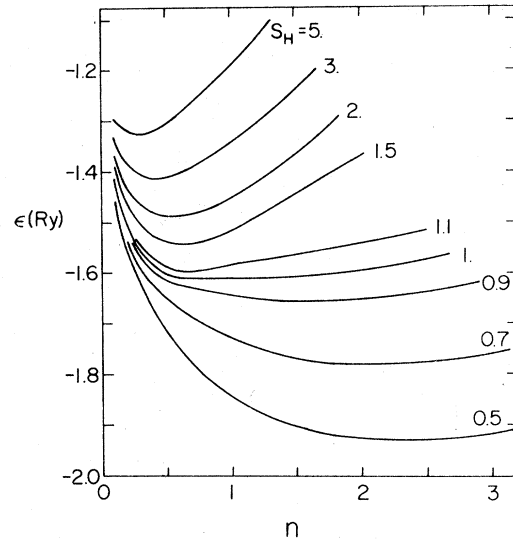


FIG. 2. EHD energy per pair ϵ vs density n (units of 10^{17} cm^{-3}) for the model exchange-correlation energy E_{xc}^0 . S_H , the stress splitting of the valence band at $k=0$, is given in meV. S_H (meV) = $0.364 \times$ the applied $\langle 111 \rangle$ stress (kg/mm^2).

from experiment⁵ to be 2.8. The exchange-correlation energy was taken in the two approximations E_{xc}^0 and E_{xc}^∞ as described in Sec. II. The published numerical correlation energies^{3,15} were smoothed to remove noise due to roundoff and then interpolated by a cubic spline method.

The resulting EHD energy per pair for the model exchange-correlation energy E_{xc}^0 is plotted against

TABLE II. Calculated behavior of the EHD in Ge under $\langle 111 \rangle$ uniaxial stress. 1 Ry = 2.655 meV.

S_H (meV)	n (10^{17} cm^{-3})	ϵ_g	E_{xc}^0	$E_F(E)$ (Ry)	$E_F(H)$	E_{xc}^∞	ϵ_g (Ry)
0	2.53	-2.36		1.0	1.54	3.52	-2.59
0.25	2.48	-2.14		1.17	1.57	3.47	-2.37
0.50	2.32	-1.93		1.32	1.55	3.32	-2.15
0.75	1.99	-1.75		1.40	1.45	3.05	-1.95
0.95	1.43	-1.63		1.36	1.23	2.70	-1.81
1.0	0.69	-1.61		1.05	0.83	2.57	-1.78
1.15						1.99	-1.69
1.2	0.67	-1.58		1.04	0.86	0.90	-1.68
1.5	0.64	-1.54		1.00	0.88	0.87	-1.63
2.0	0.56	-1.49		0.91	0.90	0.80	-1.57
2.5	0.47	-1.45		0.82	0.90	0.71	-1.52
3.0	0.42	-1.41		0.76	0.90	0.62	-1.48
4.0	0.34	-1.36		0.66	0.89	0.53	-1.41
5.0	0.27	-1.32		0.57	0.87	0.45	-1.36
6.0	0.22	-1.30		0.50	0.83	0.38	-1.33
8.0	0.14	-1.27		0.36	0.70	0.29	-1.28
10.0	0.12	-1.26		0.32	0.66	0.24	-1.25

density for various values of stress in Fig. 2, where S_H is given in meV. As the stress increases, the minima of the curves shift to higher energy and to lower density. To locate the minima accurately we found it to be more efficient to look for the zeros of $p = -(\partial E/\partial V)_N$ than to use the equivalent procedure of finding the minimum of $\epsilon(n)$ directly. The results from the two methods are the same. Representative numerical values are given in Table II.

In Fig. 2, for stresses in a very narrow range about $S_H = 1$ meV the $\epsilon(n)$ curve is almost flat in the vicinity of the minimum over a large range of density values (this flat region extends over almost a factor 2 in density). Such a flattening is also found for the model exchange-correlation energy E_{xc}^∞ but in this case at the value of stress corresponding to $S_H = 1.2$ meV. In both models the effect is found at the value of stress at which the hot valleys are just emptied of electrons as the stress is increased. Also in both models the presence of a very weak local maximum in the energy was possible numerically in the "flat" region. The presence of such a local maximum [which would imply a double minimum in the $\epsilon(n)$ curve] would be very interesting since the density of the EHD would decrease discontinuously and by a large amount as the value of the applied stress is increased through the critical value at which the hot valleys are emptied. However, any such energy feature is too weak for us to draw reliable conclusions about such a phenomenon from the present theory. Whether or not a more detailed calculation would give such discontinuous behavior, at least a very sharp change in the EHD density with stress is to be expected.

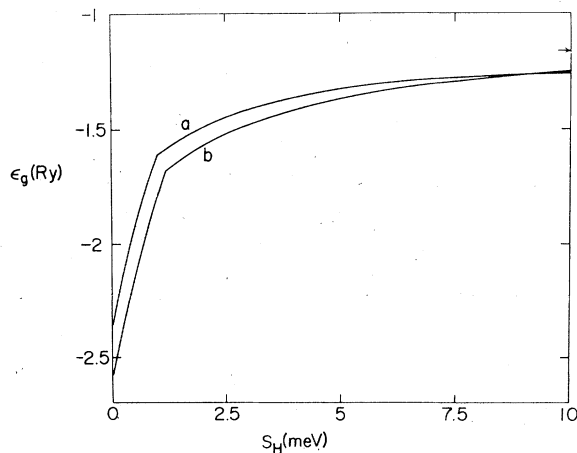


FIG. 3. EHD ground-state energy per pair, ϵ_g , vs stress splitting S_H of the valence band. Curves *a* and *b* correspond to the exchange-correlation energies E_{xc}^0 and E_{xc}^∞ , respectively.

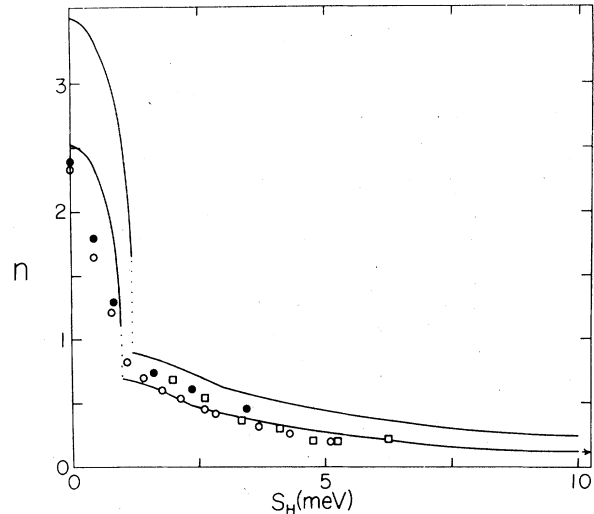


FIG. 4. EHD density n (10^{17} cm^{-3}) vs S_H . The higher- and lower-density curves correspond to E_{xc}^∞ and E_{xc}^0 , respectively. The dotted portions indicate the region of very rapid or discontinuous change of density with stress which is due to the emptying of the hot valleys of electrons. The experimental data: \square , Ref. 4; \bullet , Ref. 5; \circ , Ref. 6. The limiting value of Vashishta *et al.* (Ref. 3) is arrowed.

The numerical work was carried out to an accuracy better than $\frac{1}{4}\%$. A similar numerical accuracy was quoted in the evaluation of the correlation energy in Refs. 3 and 15. The main uncertainty in the calculation arises from our lack of a precise knowledge of the experimental valence-band parameters and more importantly of the exchange-correlation energy.

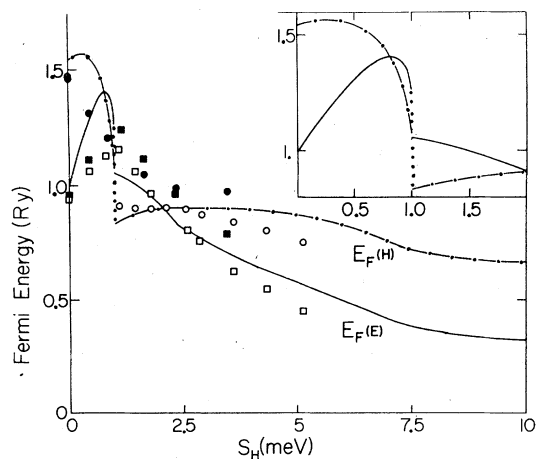


FIG. 5. Electron and hole Fermi energy (solid and dashed lines, respectively) vs stress splitting of the valence band S_H for the model exchange-correlation energy E_{xc}^0 . \circ (Ref. 6) and \bullet (Ref. 5) are experimental hole Fermi energies; \square (Ref. 6) and \blacksquare (Ref. 5) are experimental electron Fermi energies.

In Fig. 3 we show ϵ_g the ground-state energy per pair of the EHD plotted against stress for the two model exchange-correlation energies. Notice the abrupt change in slope of the curves at the value of stress at which the hot valleys are just emptied.

The EHD density is plotted against stress for the two exchange-correlation energy models together with the available experimental data in Fig. 4. In addition to the already discussed abrupt change in density at $S_H = 1$ meV for the model E_{xc}^0 (lower-density curve) and at $S_H = 1.2$ meV for E_{xc}^∞ (higher-density curve) there is a sudden change in slope which occurs when $S_H = E_F(H)$, i.e., when N_+ becomes zero. Both models reproduce well the general behavior of the experimental data, and the model E_{xc}^0 gives good quantitative agreement with experiment at all stresses for which data is available. However, more detailed experimental results in the vicinity of $S_H = 1$ meV are needed to test the theory in that interesting region. Notice that the density computed from the large-stress model exchange-correlation energy E_{xc}^∞ which corresponds to only one electron and one hole band populated remains significantly larger than the experimental values even when only one hole band remains populated ($S_H \geq 2.9$ meV). This may be an indication that valence-band nonparabolicity, warping, and coupling continue to have a role in the exchange-correlation energy in this region of stress values.

The electron and hole Fermi energies for the model E_{xc}^0 are shown in Fig. 5. Note that at low stress the calculated electron and hole Fermi en-

ergies both increase initially with increasing stress and then decrease abruptly near $S_H = 1$ meV. As the stress increases further the hole Fermi level continues to rise until the population of the (+) hole band decreases to zero at $S_H = 2.4$ meV. At that value of stress the slope of the $E_F(E)$ curve changes, and further reduction of the calculated electron and hole Fermi energies with increasing stress is due to the decreasing influence of valence-band nonparabolicity on the hole kinetic energy.

The experimental data clearly shows the initial rise of the electron Fermi level at low stress, and also the near independence of the hole Fermi level of stress in the region of intermediate stress which is given by our calculation. However, in the region near $S_H = 1$ meV the discrepancy between the two sets of experimental data (particularly for the hole Fermi energy) is large and at the present time it is not possible to judge whether the above abrupt changes do indeed occur as predicted. A more detailed experimental study of this region would be very desirable.

ACKNOWLEDGMENTS

We wish to thank J. Bajaj, H.-h. Chou, L. Liu, and G. Wong for many useful discussions and R. S. Markiewicz for a communication. This work was supported in part under the NSF-MRL program through the Material Research Center of Northwestern University (Grant No. DMR 76-80847) and in part by the NSF under Grant No. DMR 77-09937.

¹M. Combescot and P. Nozières, *J. Phys. C* **5**, 2369 (1972).

²W. F. Brinkman and T. M. Rice, *Phys. Rev. B* **7**, 1508 (1973).

³P. Vashishta, P. Bhattacharyya, and K. S. Singwi, *Phys. Rev. B* **10**, 5108 (1974).

⁴B. J. Feldman, H.-h. Chou, and G. K. Wong, *Solid State Commun.* **26**, 209 (1978).

⁵G. A. Thomas and Ya. E. Pokrovskii, *Phys. Rev. B* **18**, 864 (1978).

⁶H.-h. Chou and G. K. Wong, *Phys. Rev. Lett.* **41**, 1677 (1978).

⁷H.-h. Chou, G. K. Wong, and B. J. Feldman, *Phys. Rev. Lett.* **39**, 959 (1977).

⁸B. J. Feldman, H.-h. Chou, and G. K. Wong, *Solid State Commun.* **28**, 305 (1979).

⁹H.-h. Chou, J. Bajaj, and G. K. Wong, *J. Lumin.* **18-19**, 131 (1979).

¹⁰G. Kirczenow and K. S. Singwi, *Phys. Rev. Lett.* **41**, 326 (1978); **41**, 1140 (E) (1978).

¹¹R. S. Markiewicz and S. M. Kelso, *Solid State Commun.* **25**, 275 (1978).

¹²L. Liu, *Solid State Commun.* **25**, 805 (1978).

¹³G. E. Pikus and G. L. Bir, *Sov. Phys. Solid State* **1**, 136 (1959).

¹⁴J. C. Hensel and K. Suzuki, *Phys. Rev. B* **9**, 4219 (1974).

¹⁵P. Bhattacharyya, V. Massida, K. S. Singwi, and P. Vashishta, *Phys. Rev. B* **10**, 5127 (1974).

¹⁶L. Liu and L. S. Lui, *Solid State Commun.* **27**, 801 (1978).